Amphiphilic Antifogging/Anti-Icing Coatings Containing POSS-PDMAEMA-b-PSBMA
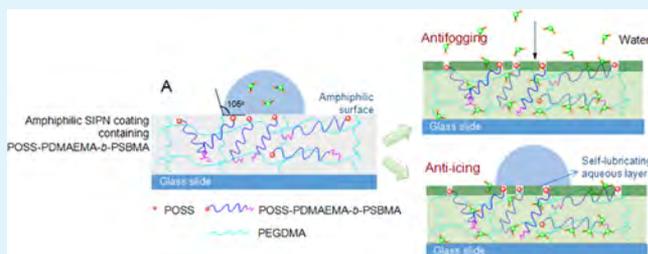
Chuan Li, Xiaohui Li, Chao Tao, Lixia Ren, Yunhui Zhao, Shan Bai, and Xiaoyan Yuan*

School of Materials Science and Engineering, and Tianjin Key Laboratory of Composite and Functional Materials, Tianjin University, Tianjin 300072, China

S *Supporting Information*

ABSTRACT: Highly transparent antifogging/anti-icing coatings were developed from amphiphilic block copolymers of polyhedral oligomeric silsesquioxane-poly[2-(dimethylamino)-ethyl methacrylate]-*block*-poly(sulfobetaine methacrylate) (POSS-PDMAEMA-b-PSBMA) with a small amount of ethylene glycol dimethacrylate (EGDMA) via UV-curing. The excellent antifogging properties of the prepared coatings were originated from the hygroscopicity of both PDMAEMA and PSBMA blocks in the semi-interpenetrating polymer network (SIPN) with polymerization of EGDMA and hydrophobic POSS clusters aggregated on the surface. PDMAEMA with a lower critical solution temperature and PSBMA with an upper critical solution temperature in the block copolymers facilitated dispersion and absorption of water molecules into the SIPN coatings, fulfilling the enhanced antifogging function. Analysis of differential scanning calorimetry further confirmed that there was bond water and nonfreezable bond water in the SIPN coatings. The amphiphilic SIPN coatings exhibited the anti-icing ability with a freezing delay time of more than 2 min at −15 °C, owing to the aggregation of hydrophobic POSS groups and the self-lubricating aqueous layer generated by nonfreezable bond water on the surface. The prepared transparent antifogging/anti-icing coatings could have novel potential applications in practice.

KEYWORDS: *amphiphilic coating, semi-interpenetrating polymer network, POSS, antifogging, anti-icing*

INTRODUCTION

Formation of fog is ascribed to condensed water droplets caused by unexpected changes in temperature and humidity, bringing about optical opacity of transparent surfaces such as windshields, periscopes, and display devices in the analytical instruments.[1−3] To alleviate the trouble of fog, super-hydrophilic polymer films have been extensively investigated because their surfaces can quickly absorb and spread condensed water droplets, forming a continuous aqueous layer that allows light to pass through without too much scattering.[2−5] Superhydrophobic surfaces were also applied to mitigate fogging problems and impart to these surfaces an antifogging performance.[6,7] Nevertheless, the preparation of highly transparent antifogging coatings still remained a challenge, especially because of the meticulous preparation process of the superhydrophilic and superhydrophobic surfaces with micro-/nano-structures, which possibly limited their applications.[5−7]

In the recent years, amphiphilic coatings have been developed to achieve effective antifogging properties via the synergistic strategy of hydrophilic and hydrophobic components.[3,8−10] Cohen et al. prepared zwitter-wettable antifogging coatings by layer-by-layer assembly from chitosan and Nafion with a nanoscale-thin hydrophobic capping layer, enabling water vapor to diffuse rapidly into the underlying hydrophilic coatings.[8] Triggered by the hydrophilic/hydrophobic balance, Ming et al. fabricated a semi-interpenetrating polymer network

(SIPN) coating from an acrylate copolymer, namely, poly(2-(dimethylamino)-ethyl methacrylate-*co*-methyl methacrylate), via polymerization of ethylene glycol dimethacrylate (EGDMA) to achieve antifogging.[9,10] In contrast to superhydrophilic or superhydrophobic antifogging coatings, amphiphilic coatings displayed high initial water contact angles (CAs), which subsequently decreased to low values within a period of time.[8,9] Water or vapor molecules could be rapidly absorbed from the surrounding environment and spread in the coatings by a hydrogen-bond interaction in the form of nonfreezable water, rather than condensed as drops of liquid water on the surface.[2−4,8−10] The hydrophobicity of amphiphilic coatings also facilitated dispersion of water molecules into the coatings.[3,8−10]

In addition to the antifogging capability, the amphiphilic coatings exhibited frost-resistance[3,10] or anti-icing properties.[11,12] For example, a small amount (1 wt %) of amphiphilic copolymer poly(dimethylsiloxane) (PDMS)-poly(ethylene glycol) (PEG, 25%) was introduced in the smooth PDMS coating and then a viscous lubricating liquid-like layer could generate at the coating surface, which exhibited icephobicity with a lower ice adhesion strength.[11] Amphiphilic cross-linked hyper-
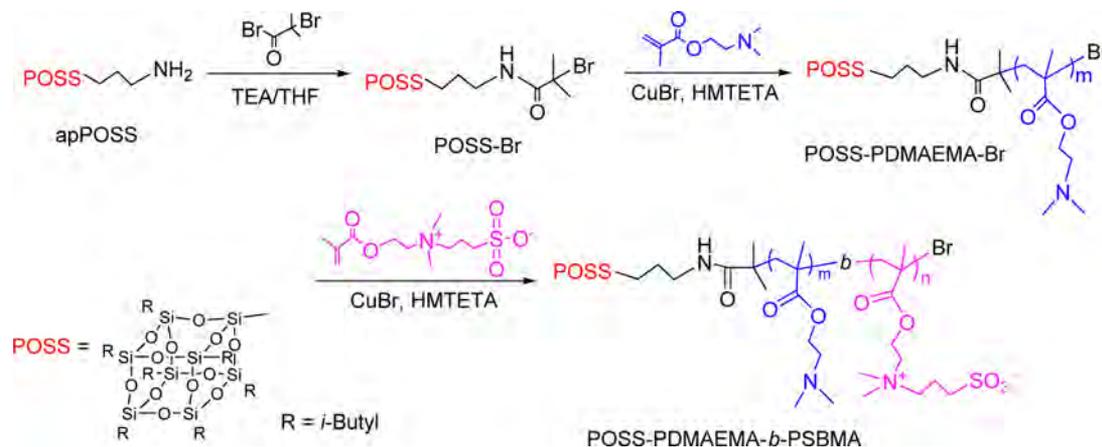
Scheme 1. Schematic Illustration of the Synthesis of POSS-PDMAEMA-*b*-PSBMA

Table 1. Compositions of the Prepared Block Copolymers

sample	feeding composition DMAEMA/SBMA (mol/mol)	molar composition DMAEMA/SBMA in the copolymer[a] (mol/mol)	$\bar{M}_n{}^a$ ($\times 10^4$)	PDI
POSS-D$_{50}$-*b*-S$_7$	50:7	43:7 (6.14:1)	0.97	1.07
POSS-D$_{70}$-*b*-S$_{10}$	70:10	65:11 (5.91:1)	1.43	1.08
POSS-D$_{90}$-*b*-S$_{13}$	90:13	95:15 (6.33:1)	2.02	1.11
D$_{50}$-*b*-S$_7$	50:7	40:11 (3.64:1)	0.96	1.19

[a]The molar composition and the number-average molecular weight of the POSS-PDMAEMA-*b*-PSBMA block copolymers (abbreviated as POSS-D$_{50}$-*b*-S$_7$, POSS-D$_{70}$-*b*-S$_{10}$, and POSS-D$_{90}$-*b*-S$_{13}$, respectively) were estimated by ^{1}H NMR spectra, and the result of PDMAEMA-*b*-PSBMA (abbreviated as D$_{50}$-*b*-S$_7$) was determined by GPC.

branched fluoropolymers containing water-absorbing PEG chains also demonstrated anti-icing properties for potential engineering applications.[12] Alternatively, the surfaces consisting of cross-linked hygroscopic polymers such as poly(acrylic acid) could be infused with water, bringing about a self-lubricating aqueous layer for the anti-icing purpose.[13,14] Moreover, slippery liquid infused nanostructured surfaces could exhibit ice-repellency behaviors,[15,16] as well as excellent optical transparency.[17] The aqueous layer self-lubricating coatings with distinguished antifogging/anti-icing abilities would exhibit a great advantage in the practical applications.[11-14]

As we know, dual-thermosensitive block copolymers can be prepared from a lower critical solution temperature (LCST) polymer such as poly(N-isopropylacrylamide) and poly(N,N-dimethylaminoethyl methacrylate) (PDMAEMA), and an upper critical solution temperature (UCST) polymer such as zwitterionic poly(sulfobetaine methacrylate) (PSBMA) or a random copolymer of poly(acrylamide-*co*-acrylonitrile).[18-20] The random or block copolymers could display both LCST and UCST characteristics in the aqueous solution,[18-20] even though they were grafted from silica nanoparticles.[18] Thus, it can be assumed that antifogging/anti-icing coatings can be developed by combining PDMAEMA with LCST and PSBMA with UCST, which could possibly give rise to a self-lubricating aqueous layer when exposed to water or vapor and synergistically enhance the antifogging and anti-icing performances. Meanwhile, PDMAEMA was chosen as the main part of the amphiphilic polymers because of its good film-forming property on substrates and fine stability. In contrast, due to strongly electrostatic and hydrogen-bond interactions with water, zwitterionic PSBMA could regulate and control the hydrophilicity of polyhedral oligomeric silsesquioxane-poly[2-(dimethylamino)ethyl methacrylate]-*block*-poly(sulfobetaine methacrylate) (POSS-PDMAEMA-*b*-PSBMA) and enhance the antifogging/anti-icing performances of the amphiphilic SIPN coatings. In addition, the zwitterionic PSBMA component could possibly reduce the freezing point of water, as stated in refs 21, 22.

According to our previous studies on POSS-containing fluorosilicone block copolymers, POSS groups with a low surface energy could migrate and aggregate on the coating surfaces, endowing them with hydrophobicity for anti-icing.[23-26] By integrating POSS with both PDMAEMA and PSBMA via atom transfer radical polymerization (ATRP), in this work, we prepared the amphiphilic SIPN coatings from POSS-PDMAEMA-*b*-PSBMA block copolymers with a small amount (10 wt %) of EGDMA via UV-curing. We supposed that PDMAEMA and PSBMA blocks in the cross-linked PEGDMA network coupled with hydrophobic POSS groups could facilitate absorption of water or vapor molecules into the coatings to enhance the antifogging performance. In addition, the amphiphilic SIPN coating was expected to decrease the water freezing-point by forming a self-lubricating aqueous layer at the surface so as to keep high transmittance under foggy conditions and display the anti-icing properties.

EXPERIMENTAL SECTION

Synthesis of POSS-PDMAEMA-*b*-PSBMA. The POSS-PDMAEMA-*b*-PSBMA block copolymers were synthesized via ATRP of DMAEMA by using POSS-Br as an initiator according to ref 27, followed by ATRP of SBMA by using POSS-PDMAEMA−Br as a macroinitiator (Scheme 1). Three POSS-PDMAEMA-*b*-PSBMA block copolymers with different polymerization degrees were prepared, whereas block copolymer PDMAEMA-*b*-PSBMA without POSS by using ethyl-2-bromoisobutanoate as the initiator was also synthesized as the control. According to the references, stronger hydrogen-bonded water molecules can form on the zwitterionic SBMA surfaces rather than on the surface of PEG,[28] and a small amount of SBMA in the PDMAEMA-*b*-PSBMA block copolymers still exhibited a dual-
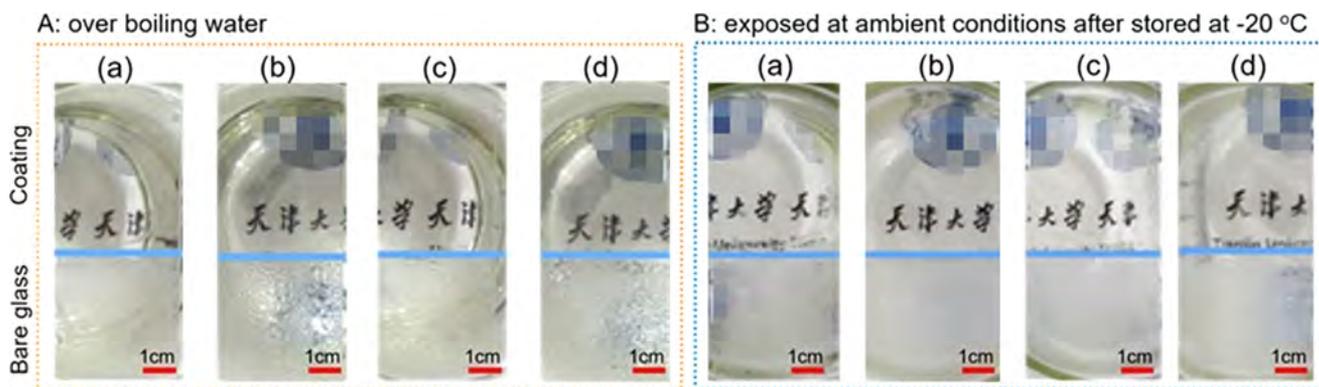
Figure 1. Photographs of the glass slides partially covered with the SIPN coatings containing POSS-D$_{50}$-b-S$_7$ (a), POSS-D$_{70}$-b-S$_{10}$ (b), POSS-D$_{90}$-b-S$_{13}$ (c), and D$_{50}$-b-S$_7$ (d), respectively, over boiling water (∼80 °C, 100% relative humidity) (A), and exposed quickly at ambient conditions (∼20 °C, 55% relative humidity) right after being stored at −20 °C for 45 min (B).

thermoresponsive performance.[20] Given that PDMAEMA chains played a key role in antifogging,[9,10] we further designed the block copolymers with a higher DMAEMA content. To obtain similar molar ratios of DMAEMA to those of SBMA, three block copolymers, that is, POSS-PDMAEMA$_{50}$-b-PSBMA$_7$, POSS-PDMAEMA$_{70}$-b-PSBMA$_{10}$, and POSS-PDMAEMA$_{90}$-b-PSBMA$_{13}$, were synthesized. Compositions of the prepared block copolymers, abbreviated as POSS-D$_{50}$-b-S$_7$, POSS-D$_{70}$-b-S$_{10}$, POSS-D$_{90}$-b-S$_{13}$ and D$_{50}$-b-S$_7$, respectively, are shown in Table 1. Detailed synthesis of the block copolymers and their characterizations by ^{1}H NMR, Fourier transform infrared (FTIR), gel permeation chromatography (GPC), and thermogravimetric analysis (TGA) are given in the Supporting Information (Figures S1−S4).

Preparation of the SIPN Coatings. A given amount of the block copolymer (POSS-D$_{50}$-b-S$_7$, POSS-D$_{70}$-b-S$_{10}$, POSS-D$_{90}$-b-S$_{13}$, or D$_{50}$-b-S$_7$) was dissolved in 2,2,2-trifluoroethanol to prepare a 25 mg/mL polymer solution. EGDMA (10 wt % based on the copolymer) and Igracure 2959 UV photoinitiator (2 wt %) were also added. The polymer coatings were prepared by casting 0.2 mL of the polymer solution onto a half of a clean glass slide (both sides) and then placing them under UV conditions (365 nm, 15 W, 1800 s) in an XL-1000 ultraviolet cross-linker apparatus for the polymerization of EGDMA. The transmittance of the SIPN coatings containing the block copolymers, POSS-D$_{50}$-b-S$_7$, POSS-D$_{70}$-b-S$_{10}$, POSS-D$_{90}$-b-S$_{13}$, and D$_{50}$-b-S$_7$, denoted as C-POSS-D$_{50}$-b-S$_7$, C-POSS-D$_{70}$-b-S$_{10}$, C-POSS-D$_{90}$-b-S$_{13}$, and C-D$_{50}$-b-S$_7$, respectively, were obtained by further air-drying at room temperature. The thickness of the obtained SIPN coatings was about 10 μm.

Characterizations. Atomic force microscope (AFM) images were obtained by a CSPM5500A microscope AFM machine (Benyuan Nano-Instruments, China) equipped with an E-type vertically engaged piezoelectric scanner and operated in a tapping-mode at room temperature. X-ray photoelectron spectroscopy (XPS) measurements were performed on a Perkin-Elmer PHI 5000C ECSA system, utilizing an excitation source of Al Kα radiation under a pressure of ∼6.7 × 10^{-6} Pa at 45°. Water CAs of the SIPN coatings and their evolution were recorded by a JC2000D CA meter (Shanghai Zhongchen Equipment Co. Ltd., China) to examine the wettability of the samples with deionized water drops (5 μL).

Antifogging Tests. The antifogging property was tested with the hot-vapor and cold−warm methods, separately. Generally, the glass slide covered by the SIPN coatings on one half of it was put over hot vapor (above about 5 cm high) by placing it on top of a glass beaker that contained hot water (∼80 °C, 100% relative humidity), and the sample transparency was recorded immediately. In addition, the appearance of the samples was recorded quickly when they were exposed to a warm, humid environment (∼20 °C, 55% relative humidity) right after being stored in a −20 °C freezer for 45 min. The transmittance of the samples was also measured in a 722s visible spectrophotometer (Shanghai Jinghua Technology Instrument Co.

Ltd., China) ranging from 400 to 800 nm for the quantitative measurement.

Anti-Icing Tests. The freezing delay time (T_D) of water droplets on the SIPN coatings was measured to test the anti-icing performance. The specimen was placed on a cold-plate (Tianjin Jing Yi Industry & Trade Co. Ltd., China), which was controlled at −15 °C. Once a deionized water droplet (5 μL) dropped on the coating surface, its appearance was recorded in every second, and the time when the water droplet became ice completely, that is, when a sharp tip appeared on the droplet top, was regarded as the freezing delay time.

Differential Scanning Calorimetry (DSC) Analysis. The bond water amount in the SIPN coatings was analyzed by DSC (TA Q2000). The samples for the DSC measurements containing a certain amount of deionized water were prepared by adding water into the SIPN coatings (about 4−5 mg), which were scraped from the glass slide. The sample was kept and stabilized in the aluminium pan for 10 days at room temperature. When no mass changes were confirmed during a period of several days, the samples were tested in the following procedure by purging nitrogen gas. The sample was first cooled from 20 to −70 °C at a cooling rate of 5 °C/min and maintained for 3 min. Then, it was heated to 20 °C at a heating rate of 5 °C/min and subsequently held at 20 °C for around 3 min. The cooling−heating cycle was also conducted in the same manner at heating/cooling rates of 10 and 15 °C/min, respectively. The total water content (W_c), the freezable water content (W_f), the nonfreezable bond water content (W_{nfb}), and the bond water content (W_b) in the samples were calculated according to the following equations.[29−33]

$$W_c = m_w/m_c \tag{1}$$

$$W_f = A_c/(334m_c) \tag{2}$$

$$W_{nfb} = W_c - W_f \tag{3}$$

$$W_b = W_{fb} + W_{nfb} \tag{4}$$

where m_w and m_c represent the masses of water and the coating, respectively, in the samples, and A_c (J/g) refers to the integral melting peak area in the heating curves. Here, we hypothesize that the enthalpies of both free and freezable water are equal to 334 J/g, the specific heat of water fusion.[29] During the analysis, the freezable bond water content (W_{fb}) was corresponding to the area of the symmetric peak at around −15 °C in the heating curves, and the free water content (W_{ff}) (that is freezable) was the difference between W_f and W_{fb} according to refs 29, 30. Therefore, the bond water content (W_b) was the sum of W_{fb} and W_{nfb}. The melting temperatures of the freezable bond water (T_{fbm}) and the freezable free water (T_{ffm}) were designated as the peak temperatures of the fitting symmetric peak and the melting peak, respectively, in the heating curves of the samples.
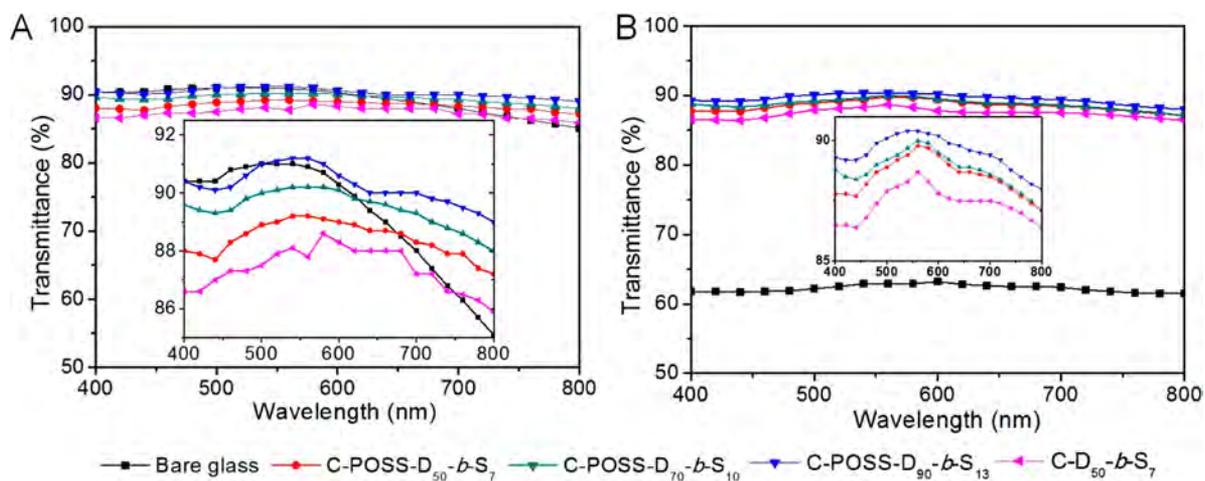
Figure 2. Transmittance of the SIPN coatings before (A) and after (B) storing at −20 °C for 45 min, and exposed quickly to a warm, humid surrounding (∼20 °C, 55% relative humidity).

RESULTS AND DISCUSSION

Antifogging Properties. The antifogging performance of the SIPN coatings was demonstrated with the hot-vapor and cold−warm methods. For the hot-vapor method, the glass slides with both sides partially coated by the SIPN coatings were placed 5 cm high above boiling water (∼80 °C, 100% relative humidity). As shown in Figure 1A, it can be seen that the uncoated areas of the bare glass slides were apparently covered by small condensed water droplets of hot vapor, resulting in optical opacity. In contrast, the other halves of the glass slides with the SIPN coatings still remained highly transparent. The excellent antifogging properties of all of the samples could be attributed to the hydrophilic PDMAEMA and PSBMA blocks in the copolymers and the cross-linked PEGDMA network, which allowed water molecules to be rapidly absorbed into the SIPN coating and possibly spread over the coating surface, similar to the situation stated in refs 8, 34. It was supposed that surface hydration of the prepared coatings could occur owing to the hydrogen-bonded inter-actions of water molecules with PDMAEMA and PSBMA blocks as well as PEGDMA.[28] When water molecules entered into the coatings, hydrogen bonds between water and polymer chains could be formed in the SIPN coatings at a molecular level due to the presence of oxygen atoms of ester and ether groups in PDMAEMA, PSBMA, and PEGDMA chains, as well as nitrogen atoms in the structure of PDMAEMA, ensuring the excellent optical transparency. Moreover, because of the electrostatic attraction of zwitterionic groups, the hydrogen-bonded interaction between hydrophilic PSBMA and water molecules is stronger than that between water and PDMAEMA or PEGDMA chains in the coatings.[28,35]

In addition, when the temperature exceeded the LCST (about 48 °C) of PDMAEMA,[20] the random coil conformation of the PDMAEMA chains tended to collapse due to the break of hydrogen-bonded interactions between the polymer and water molecules, resulting in the gathering tendency of PDMAEMA chains.[20] The PDMAEMA chains, however, were restricted by the cross-linked network and could not aggregate to some extent. Therefore, the contractive force caused by gathering of the PDMAEMA chains could give rise to free voids for dispersion of water molecules in the SIPN coatings.

The antifogging performance of the SIPN coatings was also evaluated with the cold−warm method. The SIPN coatings were first stored in a −20 °C freezer for 45 min and then rapidly exposed to a warm, humid environment (∼20 °C, 55% relative humidity). As shown in Figure 1B, the uncoated parts of the glass slides were fogged severely and the words and patterns under the container became heavily blurred due to light scattering. In contrast, the coated parts displayed high transparency, indicating the excellent antifogging performance of the SIPN coatings. When water molecules were absorbed in the coatings, hydrogen bonds between water and the polymer molecules were subsequently generated at a molecular level.[28] In addition, when the temperature was inferior to the UCST (∼5 °C) of PSBMA,[20] the random coil of the PSBMA chains tended to collapse due to the strong interchain ionic interactions between the PSBMA chains, resulting in a gathering tendency of PSBMA chains.[18−20] Therefore, water molecules were conducive to well dispersion in the SIPN coatings, which was attributed to the contractive force generated by the trend of gathering of PSBMA blocks under the limitation of the cross-linked PEGDMA structure.

The antifogging properties were quantitatively characterized by measuring the transmittance of the bare glass and the coated parts of the glass slides in the range of a visible light wavelength from 400 to 800 nm (Figure 2). The optical transmittances of C-POSS-D_{50}-b-S_7, C-POSS-D_{70}-b-S_{10}, C-POSS-D_{90}-b-S_{13}, and C-D_{50}-b-S_7 were 87.2−89.2, 88.0−90.2, 89.0−91.2, and 85.9−88.6%, respectively, which were quite similar to those of the bare glass (85.1−91.0%). The transmittance of the SIPN coatings containing POSS-PDMAEMA-b-PSBMA slightly increased with the rise of the molecular weight of the block copolymers, and all of the SIPN coatings with or without POSS exhibited minor differences in the transmittance (Figure 2A). As shown in Figure 2B, during the cold−warm antifogging test, the transmittance of the bare glass decreased sharply to about 61.5−63.2% due to the formation of fog on the surface. The transmittance of the SIPN coatings containing POSS-D_{50}-b-S_7, POSS-D_{70}-b-S_{10}, and POSS-D_{90}-b-S_{13} still remained 87.1−89.8, 87.1−90.0, and 88.0−90.4%, respectively, with trivial variations compared to the values before tests, showing an excellent antifogging performance. The SIPN coating containing D_{50}-b-S_7 without POSS became 86.4−88.7%, also exhibiting a good antifogging property but inferior to that of the coatings containing POSS-related copolymers. It was suggested that
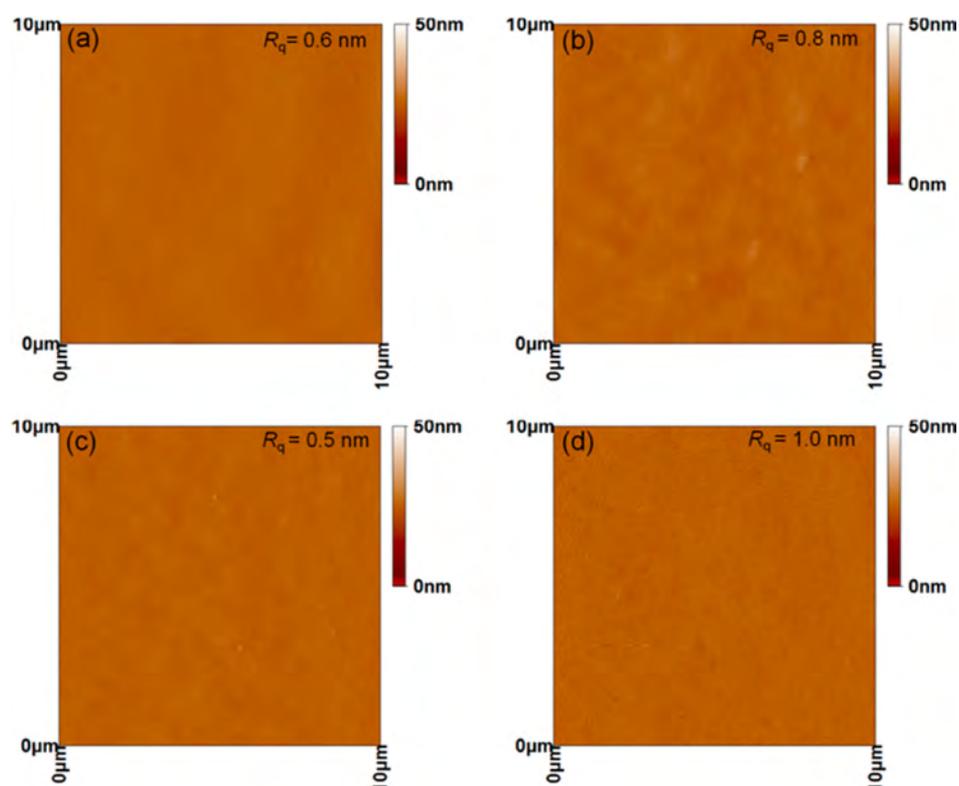
Figure 3. AFM images over a scope of 10 μm × 10 μm of the SIPN coatings containing POSS-D_{50}-b-S_7 (a), POSS-D_{70}-b-S_{10} (b), POSS-D_{90}-b-S_{13} (c), and D_{50}-b-S_7 (d).

Table 2. Surface Elemental Atomic Percentages of the SIPN Coatings Detected by XPS

sample	C 1s (atom %)	O 1s (atom %)	N 1s (atom %)	S 2p (atom %)	Si 2p (atom %)	bulk Si (atom %)
C-POSS-D_{50}-b-S_7	72.3	20.3	3.7	0.7	3.1	1.21
C-POSS-D_{70}-b-S_{10}	72.9	19.9	3.6	1.2	2.5	0.82
C-POSS-D_{90}-b-S_{13}	70.2	21.2	3.5	0.9	4.2	0.58
C-D_{50}-b-S_7	79.1	17.9	2.3	0.5		

there was an important effect of hydrophobic POSS groups on the antifogging performance of the SIPN coatings.

For different structures of the polymeric coatings with or without POSS, the C-D_{50}-b-S_7 coating exhibited low transmittance before and after fogging in comparison with C-POSS-D_{50}-b-S_7, indicating that the incorporation of POSS led to an active effect on the transmittance of the coating. It was assumed that the aggregated POSS groups on the SIPN coating surfaces could facilitate water dispersion into the amphiphilic SIPN coatings. However, for the amphiphilic SIPN coatings with similar structures, the transmittance of the coatings slightly increased before and after fogging with the rise of the molecular weight of the POSS-containing block copolymers. It was indicated that the introduction of POSS resulted in a slight negative effect on the transmittance, which did not decrease too much. It was assumed that the POSS-PDMAEMA-b-PSBMA copolymers could regulate and control the wettability of the amphiphilic SIPN coatings.

In addition, the SIPN coatings may possess the ability of "thermal remediation" because the score scratched by a clean blade could be healed by vapor. The score on the C-POSS-D_{70}-b-S_{10} coating disappeared completely when the sample was exposed over the hot vapor for 3 min, as shown in Figure S5. The phenomenon may be explained by the fact that the molecular chains of collapse could be reorganized under the

drive of water vapor due to the partially cross-linked network of the SIPN coating as well as the hydrogen-bond interactions between water and the polymeric molecules.[3,36] Moreover, the SIPN coatings demonstrated great stability when immersed in water, suggesting their long-lasting utilities, as shown in Figure S6. With the healable antifogging performance and stability, the SIPN coatings of the POSS-PDMAEMA-b-PSBMA block copolymers could have versatile potential applications.

Surface Characteristics of the SIPN Coatings. AFM was employed to observe the surface morphology of the SIPN coatings. As shown in Figure 3, all C-POSS-D_{50}-b-S_7, C-POSS-D_{70}-b-S_{10}, C-POSS-D_{90}-b-S_{13}, and C-D_{50}-b-S_7 samples exhibited smooth coating surfaces. Their root-mean-square roughness (R_q) values were estimated at ca. 0.6, 0.8, 0.5, and 1.0 nm, respectively. It was proved that an integrated film structure was successfully cross-linked by polymerization of EGDMA, endowing the SIPN coatings with preferable surface morphology.

Surface compositions of the SIPN coatings were measured by XPS. All of the element percentages on the coating surfaces, that is, C, N, O, S, and Si, are shown in Table 2. The theoretical bulk contents of the Si element, calculated from the molecular weight of the copolymers and the SIPN coating compositions, are also introduced in Table 2. It can be seen that the surface Si amounts of the amphiphilic SIPN coatings containing POSS-
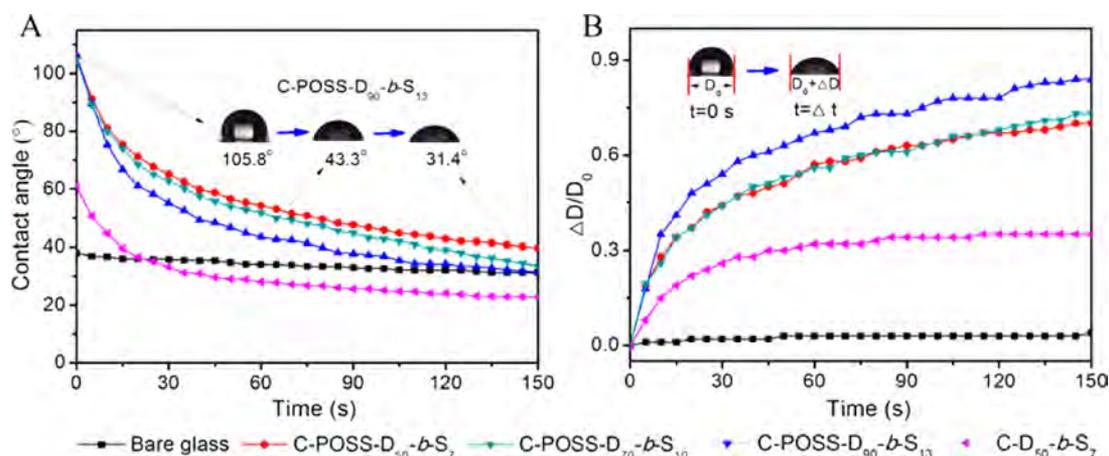
Figure 4. Variation of the water CA values on the different SIPN coatings with time in 150 s (A), and the diameter evolution ($\Delta D/D_0$) of the droplets on the coating surfaces during the recorded period (B), where $\Delta D = D - D_0$, D_0 is the original diameter ($t = 0$ s) and D is the diameter of the water droplet on the coating surface at a given time.
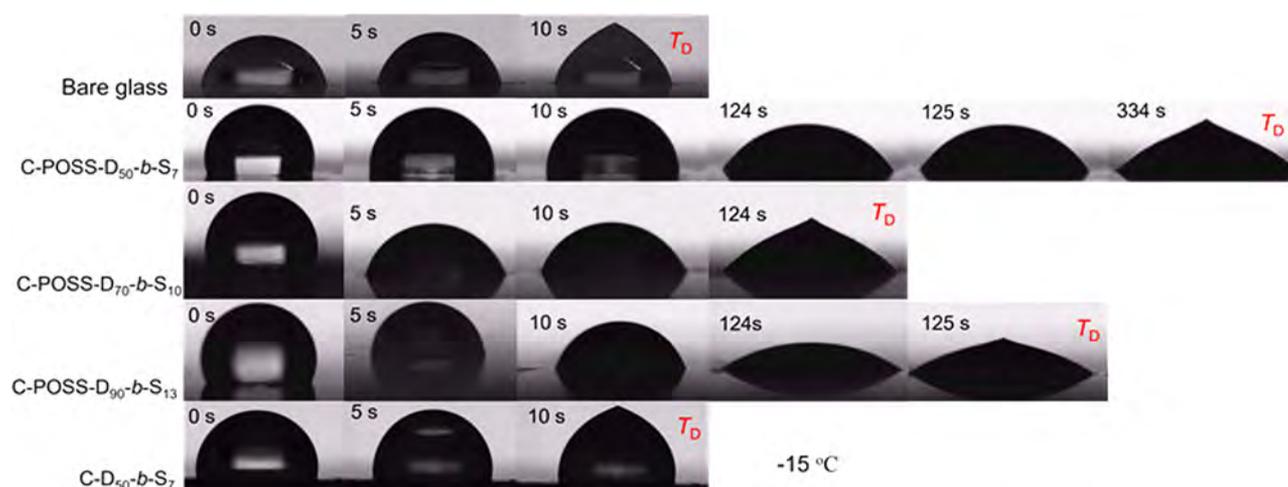

Figure 5. Optical images of the water droplets on the bare glass slide and the SIPN coatings containing POSS-D_{50}-b-S_7, POSS-D_{70}-b-S_{10}, POSS-D_{90}-b-S_{13}, and D_{50}-b-S_7 during the freezing process. The freezing delay time (T_D) of each sample was observed. The temperature of the cool-plate was controlled at −15 °C.

PDMAEMA-b-PSBMA copolymers detected by XPS were all higher than those of their bulk Si contents, respectively. It was suggested that the POSS groups could possibly aggregate on the coating surfaces due to their low surface energy and endow the SIPN surfaces with the hydrophobic property.[24−26] ATR−FTIR spectra were also applied to analyze and confirm the chemical structure of the SIPN coatings containing POSS-D_{50}-b-S_7, POSS-D_{70}-b-S_{10}, POSS-D_{90}-b-S_{13}, and D_{50}-b-S_7 block copolymers, as shown in Figure S7.

To further examine the morphology of the aggregated POSS clusters in the SIPN coatings, the samples prepared by adding a droplet of dilute copolymer solutions (1 wt % in trifluoroethanol) on copper grids and UV-curing were observed under a transmission electron microscope (TEM). As shown in Figure S8, it can be found that the aggregated POSS clusters were well dispersed within the polymer matrix with a size of 10−80 nm, which coincided with ref 37. The size of the POSS aggregates tended to decrease with the increase of the relative molecular weight of POSS-PDMAEMA-b-PSBMA due to the relative reduction of the POSS proportion in the copolymers. In fact, the size (less than 100 nm) of the POSS clusters was far smaller than the wavelength of visible light and hence the

optical properties exhibited trivial discrepancy between samples with and without POSS. Besides, the discrete POSS clusters on the coating surfaces would not affect the absorption of water molecules into the hygroscopic polymers and play an important role in regulating and controlling the dispersion of water molecules in the coatings. The POSS clusters could be analogous to the outermost layer of hollow silica nanoparticles for antifogging and antireflective thin films, as reported by Zhang.[38] Therefore, the surface structure of the C-D_{50}-b-S_7 coating lacking the POSS function was different from that of the coatings containing POSS-PDMAEMA-b-PSBMA copolymers, exhibiting a slightly lower transmittance (Figure 2B) than the latter.

Wettability of the SIPN Coatings. Changes of the water CA values of the SIPN coatings with time were recorded carefully under ambient conditions for 150 s. As shown in Figure 4A, all C-POSS-D_{50}-b-S_7, C-POSS-D_{70}-b-S_{10}, and C-POSS-D_{90}-b-S_{13} coatings exhibited high initial CA values of around 105°, whereas the initial CA value of the C-D_{50}-b-S_7 coating was about 60°. The results coincided with the recent findings in the references that an effective antifogging coating could not be superhydrophilic.[3,8−10] Particularly, the C-POSS-

D_{90}-b-S_{13} coating had a higher initial CA value (105.8 ± 0.4°), followed by a rapid decrease to 43.3 ± 1.3° in 60 s and 31.4 ± 0.7° in 150 s, which was mainly attributed to the discrete POSS clusters on the coating surface and water-absorbing polymer chains inside. During the measurement, the water CA values on all SIPN surfaces decreased rapidly in 30 s, similar to the situation of the coatings containing strongly hydrophilic polymers such as poly(vinyl alcohol)/poly(acrylic acid) and chitosan/carboxymethyl cellulose, as reported by Cohen et al.[4,8] The water CA values on all SIPN coatings decreased much more quickly at an early time due to water dispersion than water evaporation. It was suggested that water molecules could diffuse well into the SIPN coatings in a short time, similar to the results in ref 8.

To further analyze the wettability of the SIPN coatings, the diameter development of the water droplets on the coating surfaces was also calculated as shown in Figure 4B. It can be seen that the diameter of the droplet on the bare glass was almost constant during the measurement period, whereas the diameter of the water droplet on the C-D_{50}-b-S_7 coating increased by about 35%. However, the variation of the droplet diameters on the C-POSS-D_{50}-b-S_7, C-POSS-D_{70}-b-S_{10}, and C-POSS-D_{90}-b-S_{13} coatings increased by 70, 73, and 84%, respectively, demonstrating that the water droplets spread fast on the coating surfaces containing the POSS-related copolymers and dispersed well into the coatings. Moreover, the higher the polymer molecular weight, the faster the water droplet spread. Among the block copolymers, C-POSS-D_{90}-b-S_{13} with the highest molecular weight (2.02×10^4) exhibited the fastest water absorption process, whereas the SIPN coatings containing POSS-D_{50}-b-S_7 (with a molecular weight of 0.97×10^4) and POSS-D_{70}-b-S_{10} (with a molecular weight of 1.43×10^4) demonstrated similar water-dispersion speeds. Thus, the enhanced antifogging property could be caused by the strong hydrophilic blocks embedded in the cross-linked PEGDMA network and the hydrophobic POSS groups on the coating surfaces.

Anti-Icing Properties. The freezing delay time of water droplets on the SIPN coatings was recorded at −15 °C to evaluate the anti-icing properties. As shown in Figure 5, it can be observed that the SIPN coating containing D_{50}-b-S_7 showed a short freezing delay time of 10 s, that is, the water droplet became ice as quickly as it did on the bare glass. In contrast, all of the three coatings containing the POSS-PDMAEMA-b-PSBMA block copolymers presented a freezing delay time of more than 124 s, much longer than that of the C-D_{50}-b-S_7 coating without POSS. Particularly, the C-POSS-D_{50}-b-S_7 coating exhibited a longer freezing delay time of 334 s compared with C-POSS-D_{70}-b-S_{10} and C-POSS-D_{90}-b-S_{13} with similar freezing delay times of about 124 s. This phenomenon could be attributed to the following reasons. First, the POSS groups with a low surface free energy have the ability of improving the surface icephobicity as shown in POSS-containing methacrylate coatings.[24,25,39] Second, a certain amount of water molecules could be interacted with the hydrophilic PDMAEMA-b-PSBMA copolymers inside the cross-linked coatings as nonfreezable bond water through hydrogen bonds,[8−10,28] and the freezing point of water could be decreased by the zwitterionic groups of PSBMA in the coatings.[21] Finally, the POSS-PDMAEMA-b-PSBMA coating surfaces, which comprised the hydrophobic POSS groups on the coating surfaces and hydrophilic components in the SIPN coatings, could motivate the formation of a self-lubricating

aqueous layer[11,13,14] and subsequently endow the coatings with the anti-icing properties. In other words, the POSS clusters on the C-POSS-D_{50}-b-S_7 coating surface could give rise to a hydrophobic surface, whereas the hygroscopic PDMAEMA and PSBMA chains were well distributed beneath them. And then, a self-lubricating aqueous layer could form when the coating absorbed water molecules.[13,16] The surface structure of the coating is similar to the self-lubricating water layer fabricated by cross-linked hygroscopic polymers inside the micropores of silicon wafer surfaces, as put forward by Chen et al.[13] However, the hydrophilic C-D_{50}-b-S_7 coating surface without hydrophobic components could be a reservoir of water molecules rather than a self-lubricating aqueous layer.[13,16]

In fact, there were water molecules in the amphiphilic coating surfaces to maintain the presence of the self-lubricating aqueous layer.[11,13] The results of the freezing delay time for each sample exhibited a trend of decrease with the increase of the molecular weight of the copolymers. When the molecular weight of the copolymers was lower than a certain value, the total content of POSS aggregated on the coating surface would be higher, whereas the relative proportion of the hydrophilic components would drop. The freezing process of a water droplet on the bare glass and the hydrophilic C-D_{50}-b-S_7 coating without POSS presented much shorter delay times in about 10 s, very similar to the case of the general polyacrylate coating.[40] With the contribution of POSS, the C-POSS-D_{50}-b-S_7, C-POSS-D_{70}-b-S_{10}, and C-POSS-D_{90}-b-S_{13} coatings exhibited freezing delay times of more than 2 min. It could be suggested that the POSS groups played an important role in regulating and controlling superior hydrophobic/hydrophilic balance of the coating surface to form a self-lubricating aqueous layer with an anti-icing performance. Therefore, C-POSS-D_{50}-b-S_7 coating, which has the lowest content of hydrophilic units, exhibited the longest freezing delay time, whereas C-D_{50}-b-S_7 could only prevent water from freezing in a short time.

Nonfreezable Bond Water Amount in the SIPN Coatings. To further understand the antifogging/anti-icing properties of the SIPN coatings, the amounts of bond water, nonfreezable bond water, and freezable water in the coatings were analyzed by DSC. Figure 6 shows the DSC thermograms of the samples with the similar water content ($W_c \approx 1.22$) in the heating process at a rate of 10 °C/min, whereas the results of sample C-POSS-D_{90}-b-S_{13} with different water contents and the pure deionized water were also included. It can be seen that most of the melting peaks in the heating scans of the samples could be fitted into two peaks, a smaller one at around −20 to −17 °C and a sharp one at −8 to 0 °C close to the melting point of pure deionized water. The smaller and the sharp peaks could correspond to the melting enthalpies of freezable bond water (W_{fb}) and freezable free water (W_{ff}), respectively, depending on the different endothermic states in the melting process.[29,30] By quantitatively comparing the water contents in different states, we could verify the existence of the nonfreezable bond water in the SIPN coatings.[29−33]

Table 3 summarizes the water contents in different states determined by DSC. In the C-POSS-D_{50}-b-S_7, C-POSS-D_{70}-b-S_{10}, C-POSS-D_{90}-b-S_{13}, and C-D_{50}-b-S_7 coating/water binary systems, when total water content $W_c \approx 1.22$, the measured nonfreezable bond water contents (W_{nfb}) were 0.45, 0.43, 0.45, and 0.52 mg/mg, respectively, showing similar nonfreezable bond water contents in all of the SIPN coatings. In addition, the total bond water contents exhibited similar results of about 0.59−0.61 mg/mg, indicating that all of the SIPN coatings with
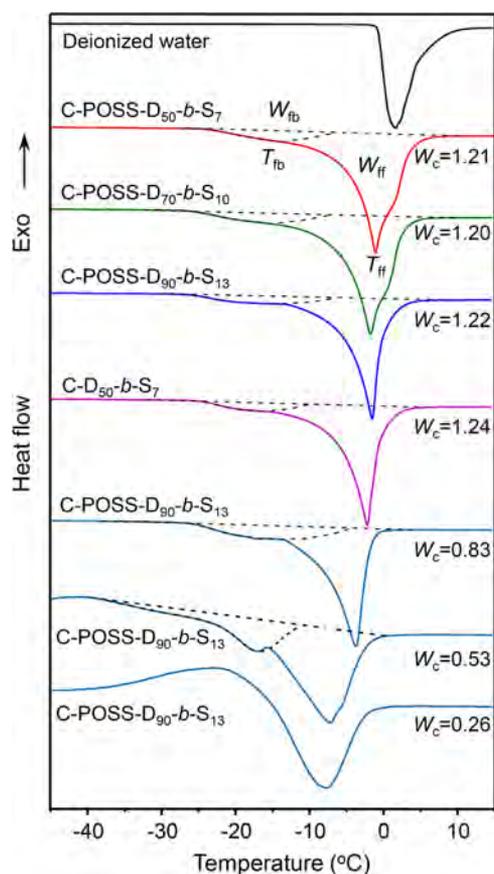
Figure 6. DSC heating curves of the SIPN coatings with a total water content (W_c) of approximately 1.22, and the sample C-POSS-D_{90}-b-S_{13} with different water contents at a heating rate of 10 °C/min. The DSC heating scan of pure deionized water was also added as a control.

or without POSS may have a similar situation of polymer—water interactions at a molecular level via hydrogen bonds.[28−33]

In addition, the DSC heating curves of C-POSS-D_{90}-b-S_{13} with different water contents are specially shown in Figure 6. We selected four W_c values, 1.22, 0.83, 0.53, and 0.26 mg/mg, for comparison. It can be seen that as the water content decreased, the melting points of the free water as well as all the contents of water in different states tended to reduce (Table 3). It was noticed that when $W_c = 0.26$, only one melting peak was detectable in the DSC heating curve, and it was difficult to distinguish the different states of water in this case. It was assumed that the smaller amount of water in the sample could possibly appear only in the state of freezable water because the

melting peak was close to the melting peak T_{ffm} values of −7 to −3 °C of other samples and higher than the T_{fbm} values of about −17 to −14 °C (Table 3).

A sufficient amount of the nonfreezable bond water in the SIPN coatings played an important role for the excellent antifogging/anti-icing properties. In fact, the nonfreezable bond water formed by the polymer—water interactions via hydrogen bonds may vary with hydrophilic polar groups and hydrophobic nonpolar groups.[41] Therefore, the similar nonfreezable bond water contents in all of the SIPN coatings was dominated by the polymeric structure, especially the hydrophilic components. In fact, the C-POSS-D_{50}-b-S_7, C-POSS-D_{70}-b-S_{10}, C-POSS-D_{90}-b-S_{13}, and C-D_{50}-b-S_7 coatings exhibited quite close nonfreezable bond water contents even when detected at different heating rates of 5, 10, or 15 °C/min, as shown in Table S1. The different heating rates exerted no significant influence on the nonfreezable bond water contents, suggesting well absorption of water in all of the SIPN coatings with or without POSS. Containing similar nonfreezable water contents, the SIPN coating with or without POSS demonstrated different antifogging/anti-icing properties, further confirming the important role of POSS on the coating surface.

The SIPN coatings, which contained POSS-PDMAEMA-b-PSBMA and comprised both low surface energy and hydrophilic blocks, endowed the surfaces with the optimum antifogging/anti-icing performances. As illustrated in Figure 7, hydrophobic POSS clusters that aggregated on the coating surfaces featured the amphiphilic surface of the SIPN coatings containing POSS-PDMAEMA-b-PSBMA block copolymers. The hygroscopic polymeric components of the coatings manipulated water molecules to disperse well into the hydrophilic matrix via hydrogen-bonded interactions. On the basis of the POSS clusters and the self-lubricating aqueous layer formed by the nonfreezable bond water on the surface, the amphiphilic SIPN coating containing POSS-PDMAEMA-b-PSBMA block copolymers exhibited excellent antifogging/anti-icing performances over the hydrophilic SIPN coating without POSS.

■ CONCLUSIONS

In this work, we developed an amphiphilic SIPN coating containing block copolymers of POSS-PDMAEMA-b-PSBMA with a cross-linked PEGDMA network. The obtained SIPN coatings that comprised both low surface energy and hydrophilic components endowed the coatings with optimal antifogging/anti-icing performances. The excellent antifogging properties were originated primarily from the hygroscopicity of PDMAEMA and PSBMA blocks embedded in the cross-linked

Table 3. Different Water Contents in the SIPN Coatings Analyzed by DSC

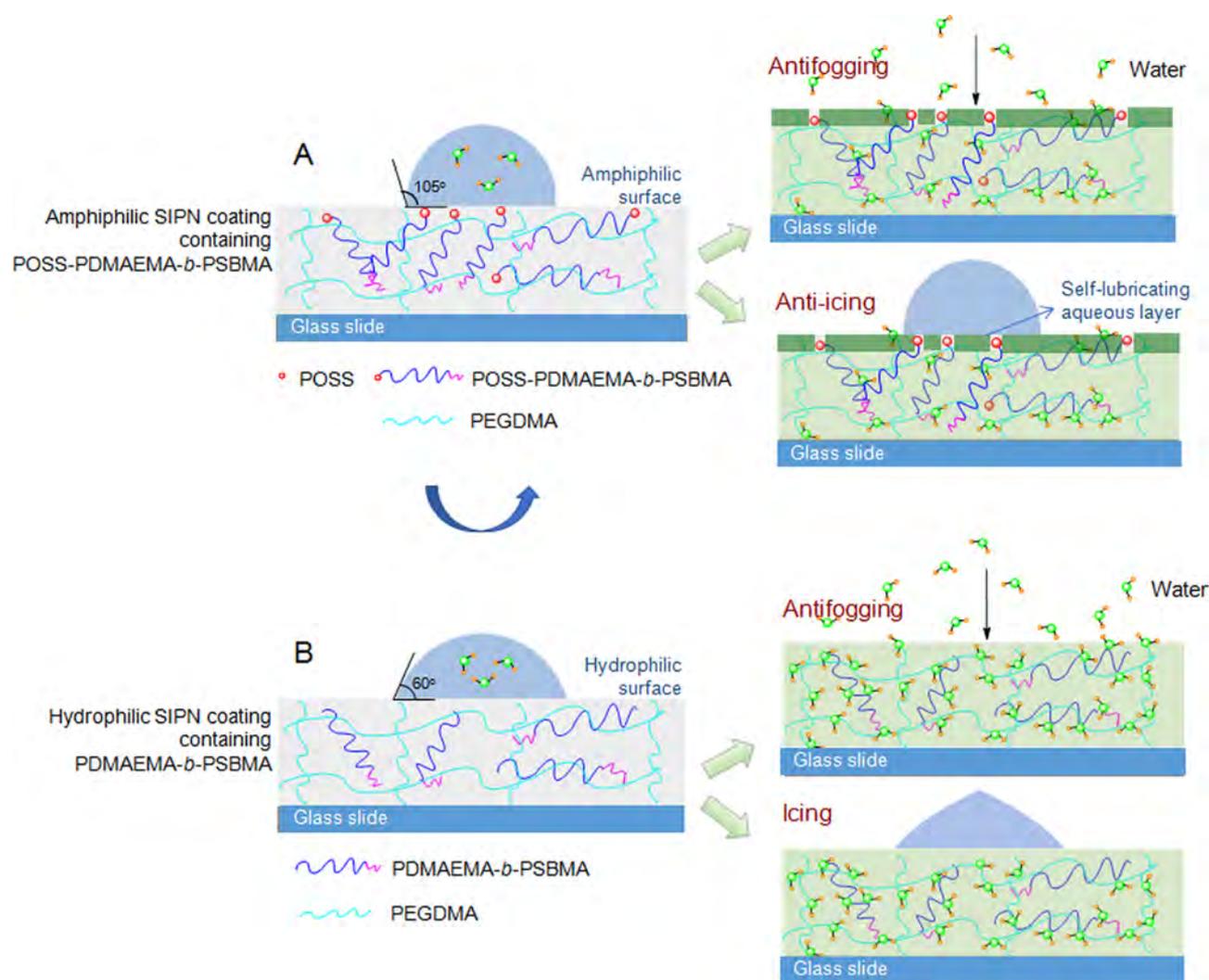| | | | freezable water | | | | | |
| | | | freezable bond water | | freezable free water | | | |
sample	W_c (mg/mg)	W_f (mg/mg)	W_{fb} (mg/mg)	T_{fbm} (°C)	W_{ff} (mg/mg)	T_{ffm} (°C)	non-freezable bond water W_{nfb} (mg/mg)	bond water W_b (mg/mg)
C-POSS-D_{50}-b-S_7	1.21	0.76	0.14	−4.01	0.62	−1.30	0.45	0.59
C-POSS-D_{70}-b-S_{10}	1.20	0.77	0.16	−17.42	0.61	−1.91	0.43	0.59
C-POSS-D_{90}-b-S_{13}	1.22	0.77	0.14	−15.01	0.63	−1.50	0.45	0.59
	0.83	0.61	0.15	−16.14	0.46	−3.35	0.22	0.37
	0.53	0.39	0.10	−16.79	0.29	−7.38	0.14	0.24
	0.26	0.26			0.26	−8.76		
C-D_{50}-b-S_7	1.24	0.72	0.09	−16.34	0.63	−2.13	0.52	0.61

Figure 7. Illustration of amphiphilic SIPN coatings containing POSS-PDMAEMA-*b*-PSBMA (A) and PDMAEMA-*b*-PSBMA (B) with a cross-linked PEGDMA network. Hydrophobic POSS aggregated on the surface and strongly hydrophilic chains distributed beneath them endowed the amphiphilic SIPN coatings with excellent antifogging/anti-icing performances in comparison with the hydrophilic SIPN coating.

PEGDMA network, as well as the hydrophobic POSS aggregated on the surface. The amphiphilic SIPN coatings with POSS groups had excellent transparency due to rapid water absorption in the coatings. PDMAEMA with LCST and PSBMA with UCST facilitated the dispersion of water molecules to enhance the antifogging behaviors. In addition, a self-lubricating aqueous layer formed by nonfreezable bond water at the surface endowed the amphiphilic SIPN coatings with great anti-icing performance, which had a freezing delay time of more than 2 min. The amphiphilic antifogging/anti-icing coatings combining POSS and PDMAEMA-*b*-PSBMA would contribute to novel potential applications in the future, such as transparent substrates in airplanes and lenses in medical instruments.

ASSOCIATED CONTENT

S Supporting Information

The Supporting Information is available free of charge on the ACS Publications website at DOI: 10.1021/acsami.7b05286.

Characterizations of the POSS-PDMAEMA-*b*-PSBMA block copolymers by ^{1}H NMR, FTIR spectra, GPC, and TGA techniques, and the characterizations of the SIPN coatings by TEM and DSC. The thermal remediation pictures of the SIPN coating by a digital camera were also presented (PDF)

AUTHOR INFORMATION

Corresponding Author

*E-mail: yuanxy@tju.edu.cn, xyuan28@yahoo.com.

ORCID

Xiaoyan Yuan: 0000-0002-2895-3730

Notes

The authors declare no competing financial interest.

REFERENCES

(1) Di Mundo, R.; D'Agostino, R.; Palumbo, F. Long-Lasting Antifog Plasma Modification of Transparent Plastics. *ACS Appl. Mater. Interfaces* **2014**, 6, 17059−17066.

(2) Wang, Y.; Li, T. Q.; Li, S. H.; Sun, J. Q. Antifogging and Frost-Resisting Polyelectrolyte Coatings Capable of Healing Scratches and Restoring Transparency. *Chem. Mater.* **2015**, *27*, 8058−8065.

(3) Li, Y. X.; Fang, X.; Wang, Y.; Ma, B. H.; Sun, J. Q. Highly Transparent and Water-Enabled Healable Antifogging and Frost-resisting Films Based on Poly(vinyl alcohol)-Nafion Complexes. *Chem. Mater.* **2016**, *28*, 6975−6984.

(4) Lee, H.; Alcaraz, M. L.; Rubner, M. F.; Cohen, R. E. Zwitter-Wettability and Antifogging Coatings with Frost-Resisting Capabilities. *ACS Nano* **2013**, *7*, 2172−2183.

(5) Zhang, J. L.; Severtson, S. J. Fabrication and Use of Artificial Superhydrophilic Surfaces. *J. Adhes. Sci. Technol.* **2014**, *28*, 751−768.

(6) Lai, Y. K.; Tang, Y. X.; Gong, J. J.; Gong, D. G.; Chi, L. F.; Lin, C. J.; Chen, Z. Transparent Superhydrophobic/Superhydrophilic TiO2-Based Coatings for Self-Cleaning and Anti-Fogging. *J. Mater. Chem.* **2012**, *22*, 7420−7426.

(7) Hikita, M.; Tanaka, K.; Nakamura, T.; Kajiyama, T.; Takahara, A. Super-Liquid-Repellent Surfaces Prepared by Colloidal Silica Nanoparticles Covered with Fluoroalkyl Groups. *Langmuir* **2005**, *21*, 7299−7302.

(8) Lee, H.; Gilbert, J. B.; Angile, F. E.; Yang, R.; Lee, D.; Rubner, M. F.; Cohen, R. E. Design and Fabrication of Zwitter-Wettable Nanostructured Films. *ACS Appl. Mater. Interfaces* **2015**, *7*, 1004−1011.

(9) Zhao, J.; Ma, L.; Millians, W.; Wu, T.; Ming, W. Dual-Functional Antifogging/Antimicrobial Polymer Coating. *ACS Appl. Mater. Interfaces* **2016**, *8*, 8737−8742.

(10) Zhao, J.; Meyer, A.; Ma, L.; Ming, W. Acrylic Coatings with Surprising Antifogging and Frost-Resisting Properties. *Chem. Commun.* **2013**, *49*, 11764−11766.

(11) Chen, D.; Gelenter, M. D.; Hong, M.; Cohen, R. E.; McKinley, G. H. Icephobic Surfaces Induced by Interfacial Nonfrozen Water. *ACS Appl. Mater. Interfaces* **2017**, *9*, 4202−4214.

(12) Zigmond, J. S.; Pollack, K. A.; Smedley, S.; Raymond, J. E.; Link, L. A.; Pavía-Sanders, A.; Hickner, M. A.; Wooley, K. L. Investigation of Intricate, Amphiphilic Crosslinked Hyperbranched Fluoropolymers as Anti-Icing Coatings for Extreme Environments. *J. Polym. Sci., Part A: Polym. Chem.* **2016**, *54*, 238−244.

(13) Chen, J.; Dou, R.; Cui, D.; Zhang, Q.; Zhang, Y.; Xu, F.; Zhou, X.; Wang, J.; Song, Y.; Jiang, L. Robust Prototypical Anti-Icing Coatings with a Self-Lubricating Liquid Water Layer Between Ice and Substrate. *ACS Appl. Mater. Interfaces* **2013**, *5*, 4026−4030.

(14) Dou, R.; Chen, J.; Zhang, Y.; Wang, X.; Cui, D.; Song, Y.; Jiang, L.; Wang, J. Anti-Icing Coating with an Aqueous Lubricating Layer. *ACS Appl. Mater. Interfaces* **2014**, *6*, 6998−7003.

(15) Wong, T. S.; Kang, S. H.; Tang, S. K. Y.; Smythe, E. J.; Hatton, B. D.; Grinthal, A.; Aizenberg, J. Bioinspired Self-Repairing Slippery Surfaces with Pressure-Stable Omniphobicity. *Nature* **2011**, *477*, 443−447.

(16) Ozbay, S.; Yuceel, C.; Erbil, H. Y. Improved Icephobic Properties on Surfaces with a Hydrophilic Lubricating Liquid. *ACS Appl. Mater. Interfaces* **2015**, *7*, 22067−22077.

(17) Yao, X.; Dunn, S. S.; Kim, P.; Duffy, M.; Alvarenga, J.; Aizenberg, J. Fluorogel Elastomers with Tunable Transparency, Elasticity, Shape-Memory, and Antifouling Properties. *Angew. Chem., Int. Ed.* **2014**, *53*, 4418−4422.

(18) Dong, Z. X.; Mao, J.; Wang, D. P.; Yang, M. Q.; Wang, W. C.; Bo, S. Q.; Ji, X. L. Tunable Dual-Thermoresponsive Phase Behavior of Zwitterionic Polysulfobetaine Copolymers Containing Poly(N,N-dimethylaminoethylmethacrylate)-Grafted Silica Nanoparticles in Aqueous Solution. *Macromol. Chem. Phys.* **2014**, *215*, 111−120.

(19) Zhang, H.; Tong, X.; Zhao, Y. Diverse Thermoresponsive Behaviors of Uncharged UCST Block Copolymer Micelles in Physiological Medium. *Langmuir* **2014**, *30*, 11433−11441.

(20) Sun, H.; Chen, X. L.; Han, X.; Liu, H. L. Dual Thermoresponsive Aggregation of Schizophrenic PDMAEMA-b-PSBMA Copolymer with an Unrepeatable pH Response and a Recycled CO2/N2 Response. *Langmuir* **2017**, *33*, 2646−2654.

(21) Chernyy, S.; Järn, M.; Shimizu, K.; Swerin, A.; Pedersen, S. U.; Daasbjerg, K.; Makkonen, L.; Claesson, P.; Iruthayaraj, J. Super-hydrophilic Polyelectrolyte Brush Layers with Imparted Anti-Icing Properties: Effect of Counter Ions. *ACS Appl. Mater. Interfaces* **2014**, *6*, 6487−6496.

(22) He, Z.; Xie, W. J.; Liu, Z. Q.; Liu, G. M.; Wang, Z. W.; Gao, Y. Q.; Wang, J. J. Tuning Ice Nucleation with Counterions on Polyelectrolyte Brush Surfaces. *Sci. Adv.* **2016**, *2*, No. e1600345.

(23) Liu, B.; Zhang, K. Q.; Tao, C.; Zhao, Y. H.; Li, X. H.; Zhu, K. Y.; Yuan, X. Y. Strategies for Anti-Icing: Low Surface Energy or Liquid-Infused? *RSC Adv.* **2016**, *6*, 70251−70260.

(24) Zhang, K. Q.; Li, X. H.; Zhao, Y. H.; Zhu, K. Y.; Li, Y. C.; Tao, C.; Yuan, X. Y. UV-Curable POSS-Fluorinated Methacrylate Diblock Copolymers for Icephobic Coatings. *Prog. Org. Coat.* **2016**, *93*, 87−96.

(25) Li, X. H.; Zhang, K. Q.; Zhao, Y. H.; Zhu, K. Y.; Yuan, X. Y. Formation of Icephobic Film from POSS-Containing Fluorosilicone Multi-Block Methacrylate Copolymers. *Prog. Org. Coat.* **2015**, *89*, 150−159.

(26) Li, B.; Li, X. H.; Zhang, K. Q.; Li, H.; Zhao, Y. H.; Ren, L. X.; Yuan, X. Y. Synthesis of POSS-Containing Fluorosilicone Block Copolymers via RAFT Polymerization for Application as Non-Wetting Coating Materials. *Prog. Org. Coat.* **2015**, *78*, 188−199.

(27) Ma, L.; Geng, H. P.; Song, J. X.; Li, J. Z.; Chen, G. X.; Li, Q. F. Hierarchical Self-Assembly of Polyhedral Oligomeric Silsesquioxane End-Capped Stimuli-Responsive Polymer: From Single Micelle to Complex Micelle. *J. Phys. Chem. B* **2011**, *115*, 10586−10591.

(28) Leng, C.; Hung, H. C.; Sieggreen, O. A.; Li, Y. T.; Jiang, S. Y.; Chen, Z. Probing the Surface Hydration of Nonfouling Zwitterionic and Poly(ethylene glycol) Materials with Isotopic Dilution Spectroscopy. *J. Phys. Chem. C* **2015**, *119*, 8775−8780.

(29) Weise, U.; Maloney, T.; Paulapuro, H. Quantification of Water in Different States of Interaction with Wood Pulp Fibres. *Cellulose* **1996**, *3*, 189−202.

(30) Nwaka, D.; Tahmasebi, A.; Tian, L.; Yu, J. The Effects of Pore Structure on the Behavior of Water in Lignite Coal and Activated Carbon. *J. Colloid Interface Sci.* **2016**, *477*, 138−147.

(31) Tahmasebi, A.; Yu, J. L.; Su, H. X.; Han, Y. N.; Lucas, J.; Zheng, H. L.; Wall, T. A Differential Scanning Calorimetric (DSC) Study on the Characteristics and Behavior of Water in Low-Rank Coals. *Fuel* **2014**, *135*, 243−252.

(32) Nakano, T.; Nakaoki, T. Coagulation Size of Freezable Water in Poly(vinyl alcohol) Hydrogels Formed by Different Freeze/Thaw Cycle Periods. *Polym. J.* **2011**, *43*, 875−880.

(33) Ostrowska-Czubenko, J.; Pieróg, M.; Gierszewska-Drużyńska, M. Water State in Chemically and Physically Crosslinked Chitosan Membranes. *J. Appl. Polym. Sci.* **2013**, *130*, 1707−1715.

(34) Zhao, J.; Meyer, A.; Ma, L.; Wang, J.; Ming, W. Terpolymer-Based SIPN Coating with Excellent Antifogging and Frost-Resisting Properties. *RSC. Adv.* **2015**, *5*, 102560−102566.

(35) Leng, C.; Hung, H. C.; Sun, S. W.; Wang, D. Y.; Li, Y. T.; Jiang, S. Y.; Chen, Z. Probing the Surface Hydration of Nonfouling Zwitterionic and PEG Materials in Contact with Proteins. *ACS Appl. Mater. Interfaces* **2015**, *7*, 16881−16888.

(36) Zhang, X.; He, J. H. Hydrogen-Bonding-Supported Self-Healing Antifogging Thin Films. *Sci. Rep.* **2015**, *5*, No. 9227.

(37) Ullah, A.; Ullah, S.; Khan, G. S.; Shah, G. M.; Hussain, Z.; Muhammad, S.; Siddiq, M.; Hussain, H. Water Soluble Polyhedral Oligomeric Silsesquioxane Based Amphiphilic Hybrid Polymers: Synthesis, Self-Assembly, and Applications. *Eur. Polym. J.* **2016**, *75*, 67−92.

(38) Zhang, X.; He, J. H. Antifogging Antireflective Thin Films: Does the Antifogging Layer Have to Be the Outmost Layer? *Chem. Commun.* **2015**, *51*, 12661−12664.

(39) Meuler, A. J.; Smith, J. D.; Varanasi, K. K.; Mabry, J. M.; McKinley, G. H.; Cohen, R. E. Relationships between Water Wettability and Ice Adhesion. *ACS Appl. Mater. Interfaces* **2010**, *2*, 3100−3110.

(40) Li, X. H.; Zhao, Y. H.; Li, H.; Yuan, X. Y. Preparation and Icephobic Properties of Polymethyltrifluoropropylsiloxane-Polyacrylate Block Copolymers. *Appl. Surf. Sci.* **2014**, *316*, 222−231.

(41) Varma-Nair, M.; Costello, C. A.; Colle, K. S.; King, H. E. Thermal Analysis of Polymer-Water Interactions and Their Relation to Gas Hydrate Inhibition. *J. Appl. Polym. Sci.* **2007**, *103*, 2642−2653.